Prostate Whole-Mount Histology Reconstruction and Registration to MRI for Correlating *in-vivo* Observations with Biological Findings

Frédéric Commandeur[1,2], Oscar Acosta[1,2], Antoine Simon[1,2], Romain Mathieu[3], Alain Fautrel[4], Khemara Gnep[1,2,5], Pascal Haigron[1,2], Renaud de Crevoisier[1,2,5]

***Abstract*— Multi-parametric magnetic resonance imaging (mMRI) is the standard exam for prostate cancer diagnosis, staging and risk assessment in current clinical routine. Correlating mMRI *in-vivo* observations with biological findings from radical prostatectomy specimen would improve the optimal therapy selection. Thus, we proposed a method for reconstructing and registering the prostate whole-mount histology (WMH) to the MRI, considering a thin slicing of the prostatectomy specimen. The method was evaluated on 3 patients, included in a prospective study, for which hematein-eosin-safran and immunohistochemistry stainings were performed. The registration error was assessed by measuring the Euclidean distance between landmarks, previously identified by an expert on both mMRI and histological slices. The mean error was 4.90 ± 1.34 mm. Our method demonstrated promising results for registering prostate WMH to *in-vivo* mMRI, thus allowing for spatial accurate correlation between radiologic observations and biological information.**

I. Introduction

In current clinical routine of prostate cancer management, the ability of accurate identification of the tumor(s) in *in-vivo* imaging and confident risk estimation is crucial for selecting the optimal therapy with patient-specific consideration. Multi-parametric magnetic resonance imaging (mMRI) has become the standard exam for non-invasive diagnosis, staging and risk assessment of prostate cancer (PCa) [1], [9]. The improvement of PCa detection and characterization using the multi-modal mMRI has been widely validated in the litterature [8], [12] by correlating prostate mMRI with prostatectomy specimen, providing the biological ground truth. These studies yielded computer-assisted diagnosis (CAD) system [6] to attend the radiologists, mainly for tumor identification, which are now familiar with tumor appearance in the different mMRI sequences, namely the T1- and T2-weigted (T1-w and T2-w) images, apparent diffusion coefficient (ADC) map and dynamic contrast-enhanced (DCE).

Different approaches were proposed to establish spatial correspondences between the mMRI and the histopathological slices. The most basic methods consisted in visual definition of spatial correspondences between prostate MRI and whole-mount histology (WMH) according to anatomical structures [13], [16]. However, this approach does not rely on an accurate spatial matching, required for robust voxel-wise analysis between biological findings and *in-vivo* observation. Registration methods have been also widely developed to map the biological information to the mMRI. Some authors proposed to identify the correspondences between MRI slides and pathological slices prior to automatic 2D registration [2], [3], [17]. The main drawbacks of this approach is the availability of 2D correspondences between prostate MRI and WMH, which may be difficult to validate due to the differences in orientations of acquisition planes in both modalities as, depicted in figure 1, in addition to the differences of thickness, the distortions and the volume loss induced by the prostatectomy resection. Devices were developed in order to improve the 2D MRI/histology matching when slicing the prostatectomy specimen [10], [11], [18], such as parallel multi-blades knifes and case-specific designed molds and guides to drive the slicing. A review of the technics proposed for improved slicing of the prostate has been proposed in [4]. However, using such devices may be not easily reproducible, as no standard protocol exists.

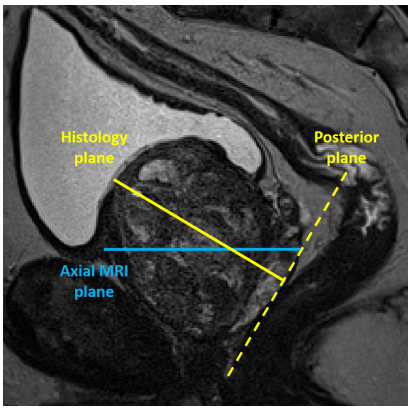

Fig. 1: T2-weighted sagittal slice showing the difference of orientation between MRI acquisition and histological slicing planes.

Other studies proposed 3D registration of the WHM to the MRI. In [15], [19], authors used respectively tissue block face photo and *ex-vivo* MRI to register the histological slices. This intermediate step allowed to reconstruct the prostate WMH and to recover the anatomy lost during the histological slicing, thus facilitating the registration with the *in-vivo* MRI. Nevertheless, these approaches do not solve the problem of nonparallel slicing and should be considered jointly with a device proposed in the litterature.

In this paper we present a framework that aims to improve the reconstruction and registration of prostate WMH to *in-vivo* MRI, by including more histological information compared to the standard anatomopathological protocol. This framework does not require devices for optimal slicing,

[1,2]Frédéric Commandeur, Oscar Acosta, Antoine Simon, Khemara Gnep, Pascal Haigron and Renaud de Crevoisier are with INSERM, U 1099, Rennes, France and Université de Rennes 1, LTSI, France.

[3]Romain Mathieu is with the Department of Urology, CHU Pontchaillou, Rennes, France.

[4]Alain Fautrel is with the H2P2 Platform, Laboratory of histopathology, Rennes, France.

[5]Khemara Gnep and Renaud de Crevoisier are also with the Department of Radiotherapy, Centre Eugène Marquis, Rennes, France.

neither intermediate image acquisitions for histological reconstruction. This work is based on a prospective study, whose final objective is to assess the feasability of correlating *in-vivo* MRI observation with biological findings.

II. Data

A total of 3 individual cases from patients with localized prostate cancer and treated with radical prostatectomy were considered. Each patient underwent an mMRI exam before the surgery. The prostatectomy specimen was then sliced by an expert pathologist according to the Stanford protocol [7], described in figure 2. The resulting blocks of histology were then embedded in paraffin. Each 0.5mm, a slice was cut using a microtome and an hematein-eosin-safran (HES) staining was performed, yielding regularly spaced and parralel tissue sections. Each 1mm, immunohistochemistry (IHC) staining were also performed, namely Ki67, CD31 and VEGF-A (vascular endothelial growth factor), for grading cells proliferation, endothelial cells and angiogenesis, respectively. All the slices were then digitalized. The figure 3 depicts an example of block slicing. Expert manual delineations were available in MRI and WMH for prostate boundaries, transition zone (TZ), peripheral zone (PZ) and urethra.

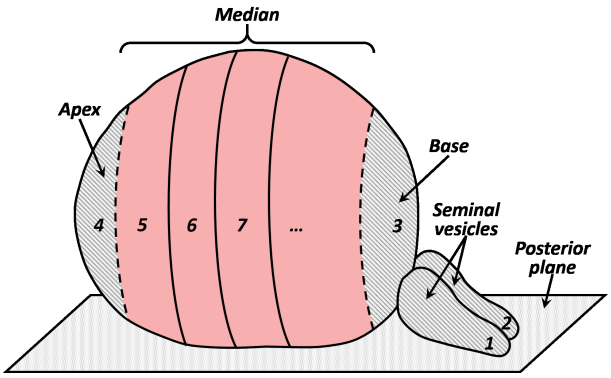

Fig. 2: Stanford protocol for the slicing of the prostatectomy specimen. In our study, we only considered median blocks. Blocks from 1 to 4, i.e. seminal vesicles, base and apex, respectively, were not used.

III. Method

The proposed framework is composed by three steps:

1) IHC/HES registration : IHC 2D images were registered to the corresponding HES image to align IHC in the spatial referential defined by HES.
2) HES/IHC Bloc-wise reconstruction : each median block obtained from the Stanford protocol was reconstructed by registering successive slices. The volume was then obtained by adding a spacing of 0.5 mm along the inferior-superior axis.
3) Simultaneous registrations to MRI : reconstructed median blocks were simultaneously registered to the MRI. MRI allowed to recover the anatomical information, namely the blocks positions and orientations, lost after prostatectomy resection and WMH processing.

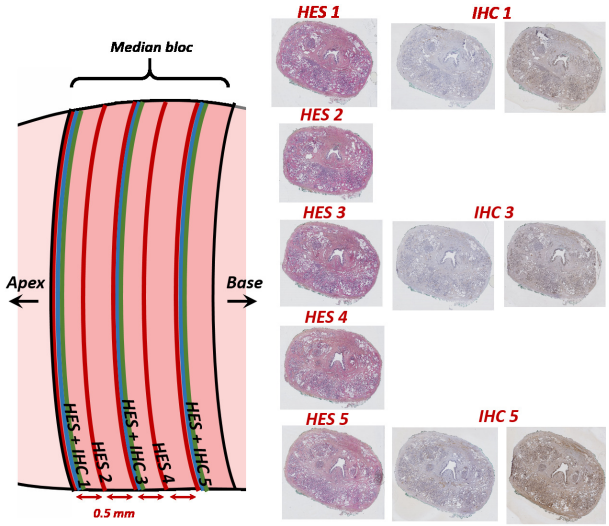

Fig. 3: Example of the slicing of a median block. Each block obtained from the median zone was paraffin-embedded and sliced using a microtome. An HES and IHC staining were performed each 0.5mm and 1mm respectively. The corresponding slices were then digitalized.

A. IHC/HES registration

Corresponding HES and IHC slices were obtained from successive samples spaced by $4\mu m$, yielding similar prostate sections. However, distortions may have appeared when cutting and putting the tissue samples on glasses. Thus, IHC images were non-rigidly registered to the corresponding HES image using the DRAMMS algorithm proposed in [14]. This method is based on the extraction of salient points in target and source images providing saliency maps. The registration is then performed to match the images according to their mutual-saliency.

B. HES/IHC block-wise reconstruction

The block-wise reconstruction framework is depicted in figure 4. It is based on the HES slides. First, RGB images were converted into grey scale images by computing at each pixel the mean of the three color channels. Secondly, each slice was rigidly registered to the successive slice using a rigid transformation and the normalized cross-correlation as similarity function. Registering the slice number n to the slice number $n+1$ provided the transform matrix $\mathscr{T}_{n,n+1}$. The inverse transform that maps the slice $n+1$ to the slice n was obtained by computing the inverse matrix $\mathscr{T}_{n+1,n} = \mathscr{T}_{n,n+1}^{-1}$. All the slices were then propagated in a common spatial referential by combining transforms, e.g. the transform $\mathscr{T}_{n,n+2} = \mathscr{T}_{n+1,n+2} \circ \mathscr{T}_{n,n+1}$ was applied to the slice n to map with the slice $n+2$, $\circ$ denoting the composition operator. IHC slices were propagated using the corresponding transforms. Finally, the block was virtually reconstructed by adding a spacing of 0.5 mm between the aligned slices along the inferior-superior axis.

C. Simultaneous block registrations to MRI

The simultaneous registrations of the blocks were performed in order to recover the anatomy of the WMH

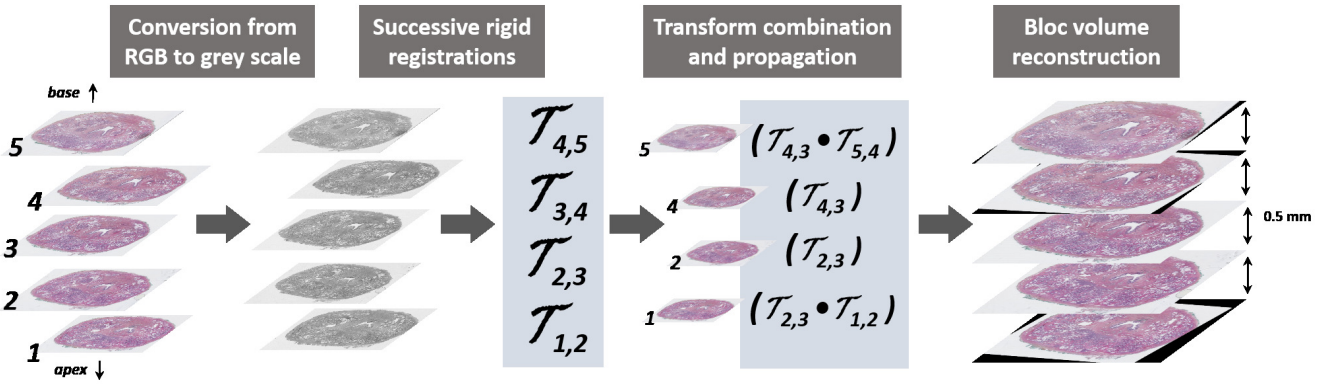

Fig. 4: Framework of the histological block-wise reconstruction. Example with a reconstructed block from 5 HES slices registered towards the slice 3. IHC were propagated with the resulting transforms.

according to the MRI, allowing for further voxel-wise MRI/biological correlation analysis. First, affine registrations were considered in order to recover block positions, block orientations and to correct the volume loss. Then, a non-rigid registration was applied to compensate for distortions due to resection and tissue slicing.

1) Affine transform: An affine transform was associated to each block, allowing for translation (block position), rotation (block orientation) and scaling (volume loss). The partial anatomical information recoverred from the block reconstructions was used to drive the registrations. Thus, we computed distance maps (DMaps) in both modalities for all the available delineation labels (i.e. prostate, TZ, PZ and urethra) using the Danielsson algorithm [5]. The DMaps were then normalized between 0 (contour points) and 1 (farthest point from the contours inside the structure). The initialization of the registration was achieved by aligning the urethra centroids along the x- and y-axis. The position along the z-axis was computed by considering prostate MRI and histological blocks thickness, K_{MRI} and $K^5_{HES},\ldots,K^N_{HES}$ respectively. An inter-block distance ε was also added between consecutive blocks due to the slicing for clinical routine analysis and estimated to 2 mm. The initial z coordinate z^n_{init} of the block n was thus computed as $z_{min}+K_{apex}+(n-4)\times\varepsilon+\sum_{k=5}^{n-1}K^k_{HES}$, where z_{min} denotes the z coordinate of the lowest point of the prostate in MRI, and K_{apex} the apex thickness defined as $K_{apex}\approx K_{base}\approx(K_{MRI}-(N-4)\times\varepsilon-\sum_{k=5}^{N}K^k_{HES})/2$. Finally, the registrations were performed by maximizing the mean squared error (MSE) between the DMaps using a standard gradient descent optimizer. Only points inside the structures were considered in the computation of the MSE. Constraints were added in the optimization procedure in order to control the transform parameters and to prohibit histological blocks overlap. After registrations, HES and IHC images were propagated.

2) Non-rigid registration: A non-rigid registration step based on B-splines transform was performed between the MRI and the 3D-WMH DMaps, in order to correct the distortions induced by the resection and the slicing of the prostatectomy specimen.

IV. Results

First, we evaluated the IHC/HES registration by measuring the resulting Euclidean distance between landmarks. These landmarks, mainly cysts and calcifications, were previously identified by an expert on both HES and IHC. Then, the proposed method was also assessed using anatomical landmarks on MRI and WMH after reconstruction/registration. IHC/HES and WMH/MRI registration results are presented in the table I. Examples of both IHC/HES and WMH/MRI registrations are depicted in figure 5.

Patients	IHC/HES errors	WMH/MRI errors
Patient 1	0.12 ± 0.08 mm	4.24 ± 1.26 mm
Patient 2	0.23 ± 0.17 mm	5.08 ± 1.42 mm
Patient 3	0.28 ± 0.13 mm	5.37 ± 1.33 mm
Mean	0.21 ± 0.13 mm	4.90 ± 1.34 mm

TABLE I: IHC/HES and WMH/MRI registration results for each patient.

V. Conclusion & Discussion

In this paper, we proposed a method to reconstruct and register the three-dimensional whole-mount prostate histology (WMH) to the *in-vivo* mMRI. Neither additional devices, proposed in the litterature to cut the prostate with accuracy according to the MRI, nor post-surgery acquisitions such as ex-vivo MRI were required. The standard clinical protocol (Stanford) combined with a refined slicing of the prostatectomy specimen allowed to partially recover anatomical information from the histological images. The three-dimensional blocks were reconstructed and simultaneously registered to the mMRI in order to recover blocks positions and orientations and to compensate the loss of volume. Finally a non-rigid registration step was used to correct the distortions induced by the histological processing. Evaluation was done according to anatomical landmarks previously identified on both modalities by an expert. Accurate matching between 3D WMH and MRI were achieved using the proposed method, with a mean final error on landmarks positions of 4.90 ± 1.34 mm. Further work will be focused on performing more robust validation, including more data and more experts for landmarks identification. The final objective is to assess the feasability of voxel-wise correlation between *in-vivo*

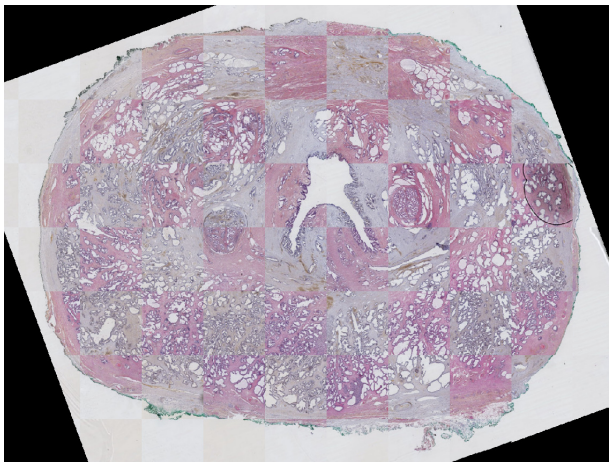

(a)

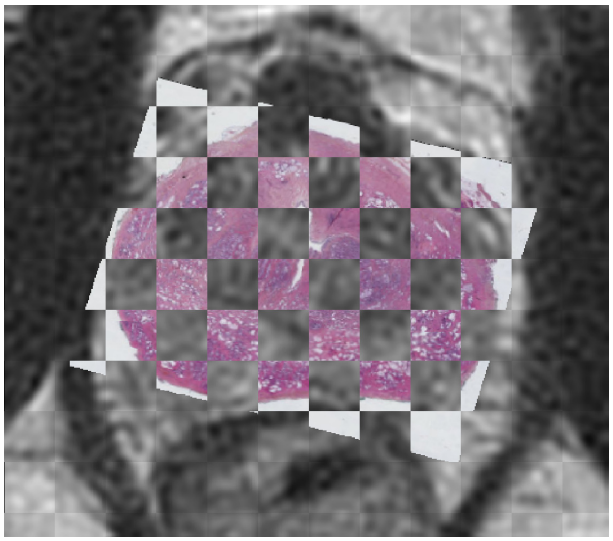

(b)

Fig. 5: Comparison of corresponding HES (pink) and Ki67 (blue) after IHC/HES registration (5(a)). Comparison of T2-w MRI and HES after WMH/MRI registration (5(b)).

radiologic observations and biological findings. Other *in-vivo* imaging modalities will be considered, such as positron emission tomography with a prostate cancer specific radiotracer 11-C choline. The establishment of these correlations is a valuable point for *in-vivo* cancer characterization at the diagnosis stage and would allow for optimal therapy selection. The accurate histology 3D reconstruction will also allow to analyse the spatial distribution of tumors, vessels and IHC and to look for correlation between vascularization, proliferation, hypoxia and aggressiveness.

ACKNOWLEDGMENT

This work was funded by the Association pour la Recherche sur le Cancer (ARC), FONDATION ARC 9 rue Guy Môquet 94803 Villejuif - France, with the project number SFI20121205882.

REFERENCES

[1] Jelle O. Barentsz, Jonathan Richenberg, Richard Clements, Peter Choyke, Sadhna Verma, Geert Villeirs, Olivier Rouviere, Vibeke Logager, and Jurgen J. Fütterer. Esur prostate mr guidelines 2012. *Eur Radiol*, 2012.

[2] J Chappelow, B Nicolas Bloch, Neil M Rofsky, Elizabeth M Genega, Robert E Lenkinski, W DeWolf, and Anant Madabhushi. Elastic registration of multimodal prostate mri and histology via multiattribute combined mutual information. *Medical Physics*, 38(4):2005–2018, 2011.

[3] J. Chappelow and A. Madabhushi. Multi-attribute combined mutual information (macmi): An image registration framework for leveraging multiple data channels. In *Biomedical Imaging: From Nano to Macro, 2010 IEEE International Symposium on*, pages 376–379, April 2010.

[4] LiHong Chen, Henry Ho, Richie Lazaro, ChoonHua Thng, John Yuen, WanSing Ng, and Chris Cheng. Optimum slicing of radical prostatectomy specimens for correlation between histopathology and medical images. *International Journal of Computer Assisted Radiology and Surgery*, 5(5):471–487, 2010.

[5] Per-Erik Danielsson. Euclidean distance mapping. *Computer Graphics and Image Processing*, 14(3):227 – 248, 1980.

[6] Leila H. Eadie, Paul Taylor, and Adam P. Gibson. A systematic review of computer-assisted diagnosis in diagnostic cancer imaging. *European Journal of Radiology*, 81(1):e70 – e76, 2012.

[7] Jonathan I. Epstein, John Srigley, David Grignon, and Peter Humphrey. Recommendations for the reporting of prostate carcinoma. *Human Pathology*, 38(9):1305 – 1309.e4, 2007.

[8] John V. Hegde, Robert V. Mulkern, Lawrence P. Panych, Fiona M. Fennessy, Andriy Fedorov, Stephan E. Maier, and Clare M.C. Tempany. Multiparametric mri of prostate cancer: An update on state-of-the-art techniques and their performance in detecting and localizing prostate cancer. *Journal of Magnetic Resonance Imaging*, 37(5):1035–1054, 2013.

[9] A. Horwich, C. Parker, T. de Reijke, and V. Kataja. Prostate cancer: Esmo clinical practice guidelines. *Ann Oncol*, 24(6):106–114, 2013.

[10] C. Hughes, O. Rouviere, F. Mege-Lechevallier, R. Souchon, and R. Prost. Robust alignment of prostate histology slices with quantified accuracy. *Biomedical Engineering, IEEE Transactions on*, 60(2):281–291, Feb 2013.

[11] S G Jhavar, C Fisher, A Jackson, S A Reinsberg, N Dennis, A Falconer, D Dearnaley, S E Edwards, S M Edwards, M O Leach, C Cummings, T Christmas, A Thompson, C Woodhouse, S Sandhu, C S Cooper, and R A Eeles. Processing of radical prostatectomy specimens for correlation of data from histopathological, molecular biological, and radiological studies: a new whole organ technique. *Journal of clinical pathology*, 58:504, 2005.

[12] Alexander P.S. Kirkham, Mark Emberton, and Clare Allen. How good is {MRI} at detecting and characterising cancer within the prostate? *European Urology*, 50(6):1163 – 1175, 2006. European Urology goes Platinum.

[13] Ronald Loch, Kathryn Fowler, Ryan Schmidt, Joseph Ippolito, Cary Siegel, and Vamsi Narra. Prostate magnetic resonance imaging: Challenges of implementation. *Current Problems in Diagnostic Radiology*, 44(1):26 – 37, 2015.

[14] Yangming Ou, Aristeidis Sotiras, Nikos Paragios, and Christos Davatzikos. Dramms: Deformable registration via attribute matching and mutual-saliency weighting. *Medical Image Analysis*, 15(4):622 – 639, 2011. Special section on {IPMI} 2009.

[15] Hyunjin Park, Morand R. Piert, Asra Khan, Rajal Shah, Hero Hussain, Javed Siddiqui, Thomas L. Chenevert, and Charles R. Meyer. Registration methodology for histological sections and in vivo imaging of human prostate. *Academic Radiology*, 15(8):1027 – 1039, 2008.

[16] Lian-Ming Wu, Xiao-Xi Chen, Han-Qing Xuan, Qiang Liu, Si-Teng Suo, Jiani Hu, and Jian-Rong Xu. Feasibility and preliminary experience of quantitative t2* mapping at 3.0 t for detection and assessment of aggressiveness of prostate cancer. *Academic Radiology*, 21(8):1020 – 1026, 2014.

[17] Gaoyu Xiao, B. Nicolas Bloch, Jonathan Chappelow, Elizabeth M. Genega, Neil M. Rofsky, Robert E. Lenkinski, John Tomaszewski, Michael D. Feldman, Mark Rosen, and Anant Madabhushi. Determining histology-mri slice correspondences for defining mri-based disease signatures of prostate cancer. *Computerized Medical Imaging and Graphics*, 35(78):568 – 578, 2011.

[18] Hidekazu Yamamoto, Dror Nir, Lona Vyas, Richard T. Chang, Rick Popert, Declan Cahill, Ben Challacombe, Prokar Dasgupta, and Ashish Chandra. A workflow to improve the alignment of prostate imaging with whole-mount histopathology. *Academic Radiology*, 21(8):1009 – 1019, 2014.

[19] Yiqiang Zhan, Yangming Ou, Michael Feldman, John Tomaszeweski, Christos Davatzikos, and Dinggang Shen. Registering histologic and {MR} images of prostate for image-based cancer detection. *Academic Radiology*, 14(11):1367 – 1381, 2007.